Research Article
Open Access
CrossMark

Hydrodynamics of laminar flow through dimpled pipes

Abstract

Laminar flow through a dimpled pipe has been investigated with a focus to determine the relationship between hydrodynamic resistance and dimple geometry. Using a periodic solution domain, in–line dimples were simulated with diameters that varied from 0.125mm to 2mm (with a pipe diameter of 6 mm). It was found that for small dimples, the flow does not enter into the dimple to forming a coherent recirculation zone. On the contrary, as the dimple diameter increases, a recirculation zone forms and moves in the downstream direction for increasing dimple size. The flow patterns within the dimple are connected to changes of hydrodynamic resistance. For dimples whose sizes are small enough to prevent recirculation, the flow resistance is constant with dimple size. Once the dimples become sufficiently large to allow recirculation, there is an inverse relationship between flow rate and pressure drop. These findings allow optimization of hydrodynamic performance when a balance between pressure drop, flow rate, and wall mass transfer is required.

Keywords: dimple geometry, pipe, recirculation, flow resistance, pressure drop, flow rate, wall mass

Volume 4 Issue 3 - 2018

John Abraham, Ryan Maki
School of Engineering, University of St. Thomas, USA

Correspondence: John Abraham, School of Engineering, University of St. Thomas, 2115 Summit Ave, St. Paul, MN 55105–1079, USA, Tel 6129-6321-69, Email jpabraham@stthomas.edu

Received: June 07, 2018 | **Published:** June 15, 2018

Introduction

An understanding of fluid flow through pipes and ducts is a fundamental requisite for the design and optimization of fluid–flow systems. In particular, the relationship between flow rate and pressure variation is critical and is among the most studied problems in fluid mechanics. Great efforts have been made to optimize fluid systems and these optimization efforts generally involve the maximization of fluid flow and/or the minimization of pressure loss. Pressure variations within piping systems are a result of so–called "friction pressure losses" and "minor pressure losses". Friction pressure losses refer to pressure drop caused by friction between the fluid and the bounding wall. Minor losses, on the other hand, are associated with pressure drop that occurs when the flow passes through some obstacles in the piping system, such as a bend, a valve, an orifice plate, a change in diameter, or other. It should be noted that "minor" losses are often significant components of pressure loss within a system. There is a design balance between minimization of pressure loss and maximization of flow that is often sought by a fluid engineer. Reasonable efforts to reduce pressure losses yet increase flow rates are of significant value for both the scientific and the engineering fields. In this regard, the present study aims at assessing the impact of dimpling on pipe walls to improve the optimal piping performance. That is, dimpled surfaces have been shown to increase hydrodynamic performance (for instance, dimpled surfaces reduce drag). Often these improvements are related to flow over external bodies and the dimples modify the boundary layer to reduce flow separation. For internal flows (i.e., flow through pipes/tubes/ducts), on the contrary, separation is not germane however the dimples still impact the flow. In fact, it has been noticed that dimpling can affect the heat/mass transfer processes between the fluid and the wall[1] and it often leads to an increase in the thermal or mass transport behavior.

The history of similar studies is rich and includes fully developed friction in coiled pipes[2] as well as the impact of dimples on external flow over flat surfaces.[3] Generally, it was found that the presence of dimples increases both the rate of heat transfer as well as the frictional pressure losses. These findings are confirmed in multiple independent studies[4–10] and are evident for a wide range of geometries and Reynolds numbers.[8] These findings are also relevant for combined force/natural convection internal flows,[11] for flows that are transitional[12] and for flows within narrow channels.[13] With the impact of dimples on the flow and heat transfer characteristics well established, some works have also turned to design optimization[14–21] and to the localized influences of the dimples on the flow patterns (both adjacent to and nearby the dimples). The ultimate goal of these studies is to find a strategy to optimize both the size and the density of dimples, to define their distribution on the tube/duct wall, and to characterize the hydrodynamic performance of dimpled tubes/ducts compared to undimpled ones.[22–29] Here, a systematic study of the pressure/flow relationship is made using numerical simulation. The study encompasses a wide range of dimple shapes. Comparisons of pressure/flow results with pre–existing solutions are made in order to establish the veracity of the solutions.

The model

For the present investigation, a circular tube with uniform dimpling is considered. The dimpling may be fabricated by a number of manufacturing processes but it is envisioned as uniform both along the length of the duct as well as around the tube perimeter. The dimples are semicircles with radius R that are formed on the tube/duct wall. Dimples are arranged uniformly around the perimeter of the duct and are not staggered in the flow direction. For the thus–described situation, the flow behavior in a short segment of duct will be repeated along the duct length. Consequently, flow periodicity can be enforced, i.e., the flow patterns through one row of dimples can be repeated through subsequent rows. The solutions are obtained using computational fluid dynamics wherein the fluid region is subdivided into a multitude of small elements over which conservation equations of mass and momentum are solved. The results presented here correspond to a laminar flow with Reynolds numbers of approximately 1150 (halfway to the onset of transitional flow and turbulence). The qualitative behavior and interpretation of the results is the same for other Reynolds numbers, provided the flow is laminar. The relevant equations are the steady state, incompressible laminar Navier Stokes

equations, including both conservation of mass and momentum. They are given below:

$$\frac{\partial u_i}{\partial x_i} = 0 \quad (1)$$

and

$$\rho\left(u_i \frac{\partial u_j}{\partial x_i}\right) = -\frac{\partial p}{\partial x_j} + \frac{\partial}{\partial x_i}\left(\mu \frac{\partial u_j}{\partial x_i}\right) \; i = 1,2,3 \; j = 1,2,3 \quad (2)$$

In these equations, the symbols ρ and μ are the fluid density and dynamic viscosity, respectively while the u_i terms are the velocities in Cartesian tensor notation, and term p represents the fluid pressure. The tube diameter is 6 mm and its length is 6 mm. The inlet and outlet of the tube are connected by periodic conditions wherein a pre–defined pressure drop across the pipe segment is specified to be 1Pa. The periodicity enforces a matching of the velocity profile at the inlet and outlet. The fluid used in the simulation was water, with a density and kinematic viscosity of 998kg/m^3 and 8.9 x 10^{-7}m^2/s, respectively. The fluid–flow equations are solved using ANSYS CFX v18.0 which is a finite volume based solution algorithm. The first calculation was performed for the no–dimple case. In this case, in fact, exact solutions for fully developed laminar flow exist and allow a validation check on the numerical results. The analytical solution, with the applied pressure drop along the pipe of 1Pa, gives a mass flow rate of 5.9g/s. The numerical results, on the other hand, give a mass flow rate of 5.8g/s, in excellent agreement.

Once the flow rate through a straight, non–dimpled tube is validated, attention is turned to the dimpled cases. Figure 1 has been prepared to illustrate the distribution of dimples around the pipe circumference. It can be noticed that eight dimples are positioned around the pipe circumference, equidistant from each other. The diameter of the dimples, indicated in Figure 1 by an annotation, is changed from 0.125mm to 2mm for different simulations. For the largest diameters, the dimples are sufficiently large to merge together and form a toroidal shape around the pipe. The follow–on figure (Figure 2) shows an oblique view of the pipe with dimples. It can be noticed that the dimples are placed midway between the inlet and outlet surfaces of the periodic segment. Once the dimensions and boundary conditions are explained, attention is turned to the computational mesh. Above–described mesh was subject to a mesh–independence test wherein the number of elements was increased and the calculations were repeated. For instance, for simulations involving a 2mm dimple, the initial mesh encompassed 282,541 elements while the refined mesh totaled 1,497,549 elements. Results obtained from the two meshes were compared to ascertain whether there was an appreciable difference. By way of example, mesh independent tests for dimples of 1 mm diameter dimples showed that the calculated flow rates differed by less than 0.3%. A similar test for 2mm diameter dimples revealed that initial mesh and refined mesh results differed by only ~1%. These results demonstrated that the initial mesh was suitable to provide results of high accuracy

More details regarding the computational mesh are provided in two further images which are shown in Figure 3. The two images focus on the mesh in a straight pipe and in a dimpled pipe near a dimple, respectively, so that the mesh deployment can easily be seen. It is seen that for both geometries, a rectangular–element mesh is deployed along the walls while tetrahedral elements are used within the core of the flow space. When a dimple is present, the wall–elements follow the dimple shape and within the dimple space itself, the elements are finer than at other locations.

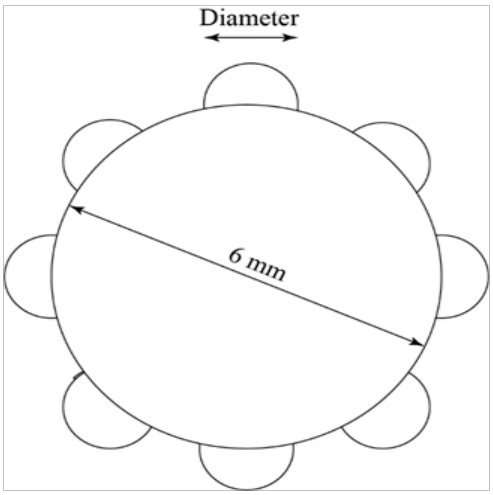

Figure 1 Illustration of the deployment of dimples around the pipe perimeter.

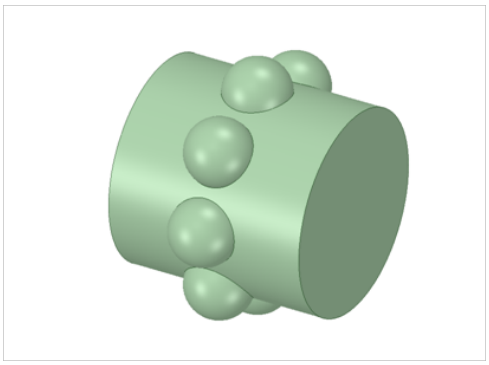

Figure 2 Oblique view showing the positioning on the dimples on the pipe exterior.

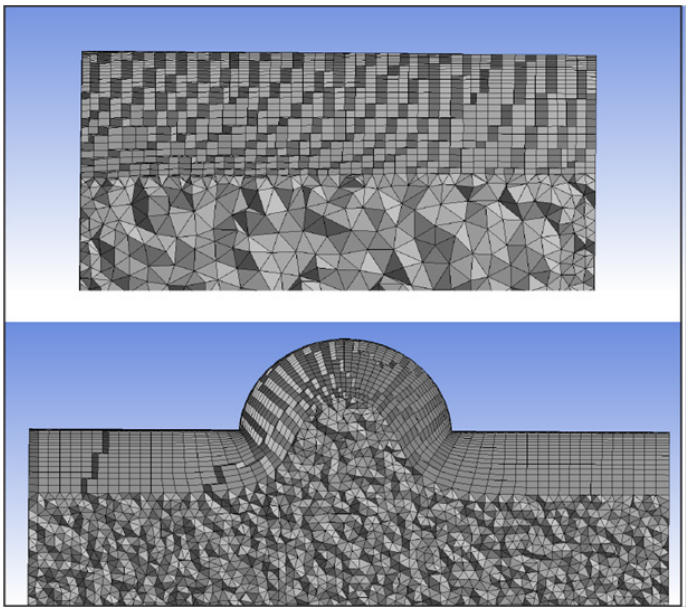

Figure 3 Distribution of elements for a straight (top image) and dimpled pipe (bottom image).

Results and discussion

The presentation of results will first focus on quantitative results and then turn toward qualitative flow patterns and their influence on the results. The primary issue to be addressed is the impact of dimples on the hydrodynamic efficiency of the pipe. Thus, for a predefined pressure drop, a comparison of flow rates through the various dimpled pipes will be made. The effect of dimple size on mass flow rate is provided in Figure 4, where dimple sizes vary from 0.125mm to a maximum of 2mm. It is found that very small dimples (0.125mm) result in a lower flow rate. As dimple sizes increase slightly, there is a more or less constant mass flow rate until the size of the dimples reaches ~1.0mm. Then, the flow begins to decrease again with dimple size. In order to explore the behavior of Figure 4, vectors of local fluid velocity are provided (Figure 5) (Figure 6). These vectors are arranged for sequentially increasing dimple sizes. It is seen that for smaller dimples, there is no coherent central eddy confined within the dimple, i.e., the dimple volume is not large enough to support a coherent eddy. To the contrary, for larger dimples (~1mm), a coherent eddy begins to form within the dimple (Figure 5). As the dimple size increases further, the recirculation patterns within the dimple become more coherent and they move downstream (Figure 6). For instance, for the largest dimple shown in Figure 6 (2mm), the center of the recirculation zone is clearly downstream of the dimple center. The off–center location is associated with a stronger fluid impact on the downstream face of the dimple and a larger stagnation pressure there. It is believed that the formation, strengthening, and movement of this recirculating flow are associated with the mass flow rate behavior displayed in Figure 4.

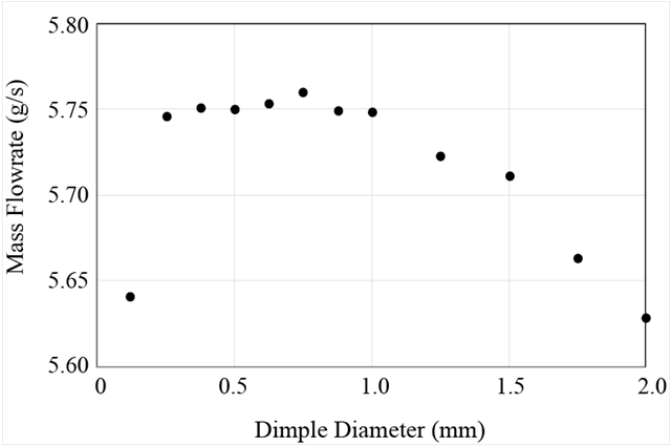

Figure 4 Effect of dimple size on mass flow rate.

It should be noted that for dimple sizes of 1mm and larger, the images show a portion of a second dimple intruding into the image. The protrusion is the semitransparent dimple walls that have become large enough to enter into the image. A deeper exploration of the hydrodynamics is provided by evaluating the pressure within the tube. Figure 7 shows the pressure along a plane that bisects the tube; the figure corresponds to a dimple size of 2mm. Flow moves from left to right in the image. It is seen that there is a large pressure (stagnation location) at the downstream face of the dimple. This location corresponds to the impact of flow against the downstream dimple surface.

A corresponding image is shown in Figure 8. There, streamlines are illustrated and they are colored according to local pressure variations along the streamline. The figure has two parts: the bottom image closely focuses on flow patterns in one of the dimples. The recirculation zone can be easily identified: it is clear that it is not centrally located within the dimple, but is rather situated downstream. Also, the pressure within the fluid in the downstream portion of the dimple exceeds that in the upstream portion – leading to the added hydrodynamic resistance. The observations obtained from Figure 4–8 provide some guidance for the design of fluid conveyance systems. It is seen that relatively large and constant flow rates can be obtained (for a predefined pressure decrease) provided that the dimples are small enough to prevent coherent eddy formation. For instance, it is possible to use dimple–walled pipes to promote mixing and mass transfer in a fluid dynamic application thus limiting the consequence of added pressure losses. Alternatively, for situations where increased pressure losses are desired, for instance in flow control applications, the dimple design should be large enough to allow the formation of the coherent recirculation region within the dimple. The quantitative results are specific to the parameters considered in the present calculations (Reynolds number, tube diameter, number of dimples deployed around the perimeter, etc.) However, the behavior of coherent recirculation within the dimple and its effect on flow rate can be generalized to other situations where these parameters differ from those presented here.

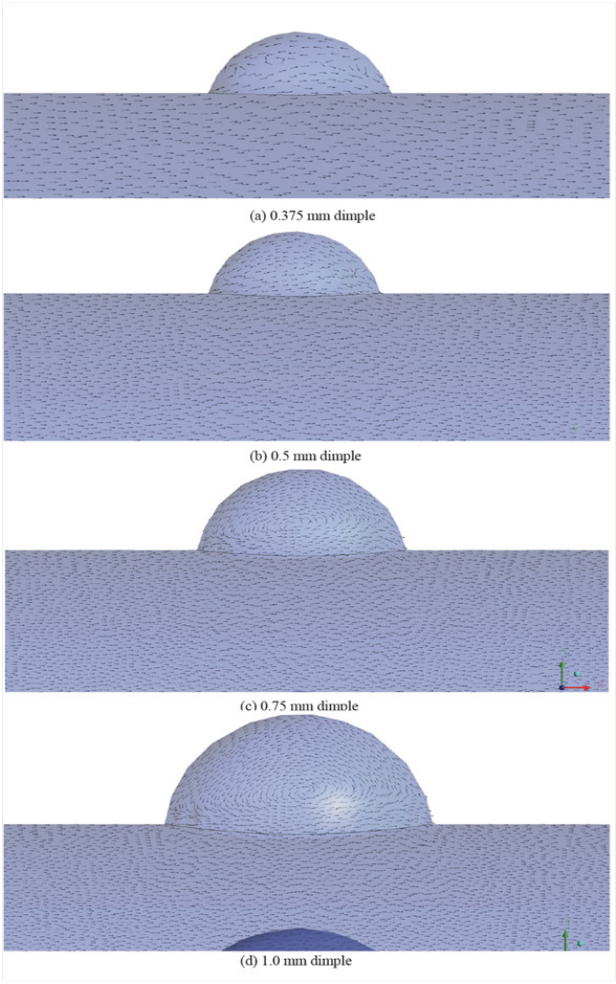

Figure 5 Changes in flow patterns with increasing dimple size (dimple sizes from 0.375 to 1.0 mm).

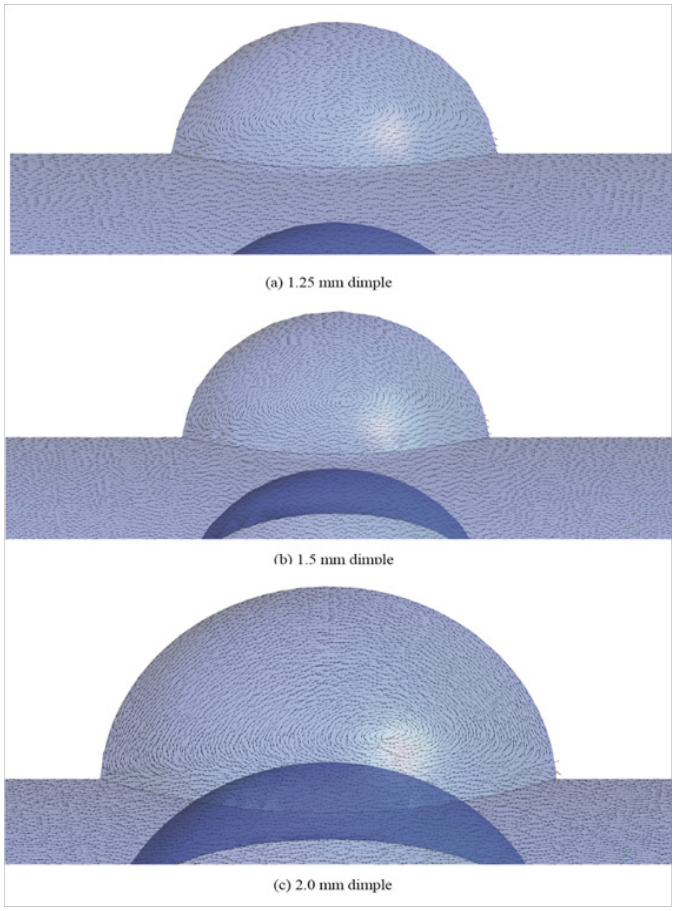

Figure 6 Changes in flow patterns with increasing dimple size (dimple sizes up to 2.0 mm).

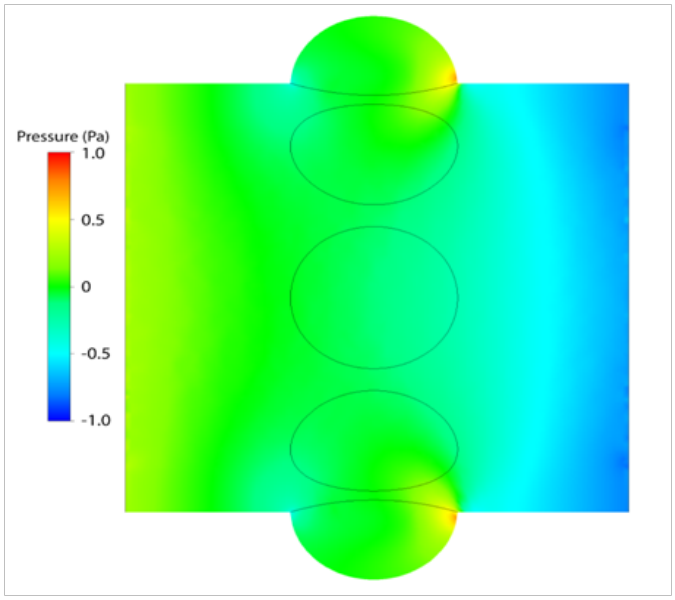

Figure 7 Pressure variation within tube and dimples, 2mm dimple size.

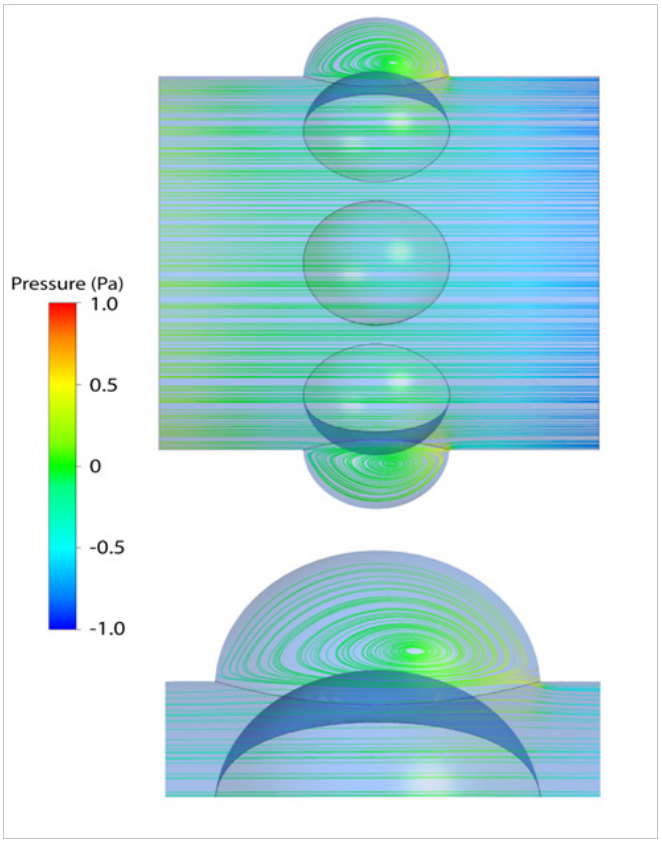

Figure 8 Pressure along streamlines, 2mm dimple size.

Concluding remarks

In this study, a three–dimensional numerical simulation of laminar flow in a dimpled pipe has been performed. The simulations accounted for dimple sizes that range from 0 mm (a smooth pipe) 2mm. It was found that the no–dimple calculations agreed very well with established laminar flow expectations. It was also found that the presence of dimples always decreased the flow compared to the smooth wall situation; however, the size of the dimple played a significant role in the flow. For very small dimples, there was a relatively large effect on the flow. On the contrary, for intermediate sized dimples, a more–or–less stable flow rate was calculated. As dimple size continued to increase, a new flow regime was established and a coherent recirculation formed within the dimple. The recirculation became more coherent as the dimple size increased and also moved downstream. The strengthening and location of the recirculation zone resulted in additional pressure losses for the flow and consequently in a decrease of flow rate.

Acknowledgements

None.

Conflict of interest

The author declares there is no conflict of interest.

References

1. Sparrow EM, Gorman JM, Friend KS, et al. Flow Regime Determination for Finned Heat Exchanger Surfaces with Dimples/Protrusions. *Numerical Heat Transfer*. 2012;63(4):245–256.
2. Austin L, Seader JD. Fully Developed Viscous Flow in Coiled Circular Pipes. *AIChE Journal*. 1973;19(1):85–94.
3. Mahmood G, Hill M, Nelson D, et al. Local Heat Transfer and Flow Structure On and Above a Dimpled Surface in a Channel. *ASME Turbo Expo Power for Land, Sea, and Air*. 2000;3:1–11.
4. Mahmood G, Sabbagh M, Ligrani P. Heat Transfer in a Channel with Dimples and Protrusions on Opposite Walls. *Journal of Thermophysics and Heat Transfer*. 2001;15(3):275–283.
5. Chen J, Müller–Steinhagen H, Duffy G. Heat Transfer Enhancement in Dimpled Tubes. *Applied Thermal Engineering*. 2001;21:535–547.
6. Ligrani P, Harrison J, Mahmmod G, et al. Flow Structure Due to Dimple Depressions on a Channel Surface. *Physics of Fluid*. 2001;13(11):3442–3451.
7. Ligrani P, Mahmood G, Harrison J, et al. Flow Structure and Local Nusselt Number Variations in a Channel with Dimples and Protrusions on Opposite Walls. *International Journal of Heat and Mass Transfer*. 2001;44(23):4413–4425.
8. Mahmood G, Ligrani P. Heat Transfer in a Dimpled Channel: Combined Influences of Aspect Ratio, Temperature Ratio, Reynolds Number, and Flow Structure. *International Journal of Heat and Mass Transfer*. 2002;45(1):2011–2020.
9. Vicente P, García A, Viedma A. Heat Transfer and Pressure Drop for Low Reynolds Turbulent Flow in Helically Dimpled Tubes. *International Journal of Heat and Mass Transfer*. 2002;45(3):543–553.
10. Burgess N, Oliveira M, Ligrani P. Nusselt Number Behavior on Deep Dimpled Surfaces Within a Channel. *ASME, Heat Transfer*. 2002;1:49–57.
11. Burgess N, Ligrani P. Effects of Dimple Depth on Channel Nusselt Numbers and Friction Factors. *Journal of Heat Transfer*. 2004;127(8):839–847.
12. Vicente P, García A, Viedma A. Experimental Study of Mixed Convection and Pressure Drop in Helically Dimpled Tubes for Laminar and Transition Flow. *International Journal of Heat and Mass Transfer*. 2002;45(26):5091–5105.
13. Zhao J, Chew Y, Khoo B. Experimental Studies on Hydrodynamic Resistance and Flow Pattern of a Narrow Flow Channel with Dimples on the Wall. *ASME, International Mechanical Engineering Congress and Exposition*. 2004;475–483.
14. Won S, Zhang Q, Ligrani P. Comparisons of Flow Structure Above Dimpled Surfaces with Different Dimple Depths in a Channel. *Physics of Fluids*. 2005;17(7):1–9.
15. Samad A, Shin D, Kim K. Surrogate Modeling for Optimization of Dimpled Channel to Enhance Heat Transfer Performance. *Journal of Thermophysics and Heat Transfer*. 2007;21(3):667–670.
16. Samad A, Lee K, Kim K. Multi–objective Optimization of a Dimpled Channel for Heat Transfer Augmentation. *Heat Mass Transfer*. 2008;45:207–217.
17. Silva C, Park D, Marotta E, et al. Optimization of Fin Performance in a Laminar Channel Flow Through Dimpled Surfaces. *Journal of Heat Transfer*. 2008;131(2):1–9.
18. Kim K, Shin D. Optimization of a Staggered Dimpled Surface in a Cooling Channel using Kriging Model. *International Journal of Thermal Sciences*. 2008;47(11):1464–1472.
19. Samad A, Lee K, Kim K. Shape Optimization of a Dimpled Channel to Enhance Heat Transfer Using a Weighted–Average Surrogate Model. *Heat Transfer Engineering*. 2010;31(13):1114–1124.
20. Kim H, Moon M, Kim K. Multi–objective Optimization of a Cooling Channel with Staggered Elliptic Dimples. *Energy*. 2011;36(5):3419–3428.
21. Li M, Khan T, Al–Hajri E, et al. Geometric Optimization for Thermal–Hydraulic Performance of Dimpled Enhanced Tubes for Single Phase Flow. *Applied Thermal Engineering*. 2016;103:639–650.
22. Saini R, Verma J. Heat Transfer and Friction Factor Correlations for a Duct having Dimple–Shape Artificial Roughness for Solar Air Heaters. *Energy*. 2008;33(8):1277–1287.
23. Xiao N, Zhang Q, Ligrani P, et al. Thermal Performance of Dimpled Surfaces in Laminar Flows. *International Journal of Heat and Mass Transfer*. 2009;52(7–8):2009–2017.
24. Wang Y, He Y, Lei Y, et al. Heat Transfer and Friction Characteristics for Turbulent Flow of Dimpled Tubes. *Chemical Engineering & Technology*. 2009;32(6):956–963.
25. Chang S, Chiang K, Chou T. Heat Transfer and Pressure Drop in Hexagonal Ducts with Surface Dimples. *Experimental Thermal and Fluid Science*. 2010;34(8):1172–1181.
26. Murugesan P, Mayilsamy K, Sursh S. Turbulent Heat Transfer and Pressure Drop in Tube Fitted with Square–cut Twisted Tape. *Chinese Journal of Chemical Engineering*. 2010;18(4):609–617.
27. Bi C, Tang G, Tao W. Heat Transfer Enhancement in Mini–Channel Heat Sinks with Dimples and Cylindrical Grooves. *Applied Thermal Engineering*. 2013;55(1–2):121–132.
28. Li M, Khan T, Al–Hajri E, et al. Single Phase Heat Transfer and Pressure Drop Analysis of a Dimpled Enhanced Tube. *Applied Thermal Engineering*. 2016;101:38–46.
29. Huang Z, Li Z, Yu G, et al. Numerical Investigations on Fully–Developed Mixed Turbulent Convection in Dimpled Parabolic Trough Receiver Tubes. *Applied Thermal Engineering*. 2017;114:1287–1299.